



Matter–curvature gravity modification and the formation of cylindrical isotropic systems

Z YOUSAF[✉]*, M Z BHATTI and H ASAD

Department of Mathematics, University of the Punjab, Quaid-i-Azam Campus, Lahore, Pakistan

*Corresponding author. E-mail: zeeshan.math@pu.edu.pk

MS received 16 December 2021; revised 25 January 2022; accepted 31 January 2022

Abstract. In this paper, we constructed the three-layered gravastar model in cylindrical space–time. We considered one of the modified gravity theories to investigate the structural progression of the celestial object. The matter we considered in this model is effective, which further constituted the perfect fluid and extra degrees of freedom due to the modification of Einstein gravity. For the modelling of the three regions of gravastar, we used a specific barotropic equation of state. We then evaluated the subsequent field equations, hydrostatic equilibrium condition and gravitational mass. Furthermore, the metric coefficients for the three regions of the system were determined. Eventually, we discussed the important features of the gravastar and deduced its physical significance along with its graphical representations.

Keywords. Self-gravitating systems; hydrodynamics; electromagnetic field; structure scalars.

PACS Nos 04.20.Cv; 04.40.Nr

1. Introduction

Stellar objects like black holes, wormholes, white dwarfs, neutron stars, etc. are the consequences of gravitational collapse. The final form of a stellar object depends upon the mass of the star that has experienced the gravitational collapse. The stellar object which draws the attention of most of the astrophysicist is the black hole. In 1916, Schwarzschild calculated the solution of general relativity (GR) field equation, presenting the concept of a black hole. By broadening the Bose–Einstein condensation concept for the construction of the new hypothetical star, a new type of solution of the Einstein field equations was introduced by Mazur and Mottola [1]. This stellar object called gravastar is considered to be distinct from a black hole. In this system, there is no event horizon and singularity.

The gravastar primarily consists of three regions. These regions are classified as interior, shell and exterior. The equation of state (EoS) of the inner region is the principal obstruction that does not encourage the gravastar to form a singularity. The energy density ρ relative to the negative pressure P is represented by the EoS $\rho = -P$. The dark energy penetration in region I reflects the presence of repulsive force on the surface of

the shell. The shell includes the effective matter accompanying the perfect fluid and isotropic pressure. The energy density ρ in this region is equal to the pressure P , i.e., $\rho = P$. In addition, the shell adds pressure to the internal area, so that the gravastar remains in hydrostatic equilibrium. The outside region is vacuumed. This shows that the pressure is negligible or zero in the region. So, for this region, the EoS $\rho = P = 0$ is recognised.

Cattoen *et al* [2] promoted the idea that there must be anisotropic pressure if there is no shell in gravastar composition. Mazur and Mottola [1] introduced gravastar representation and stated that these structures lack the event horizon and singularity. The thermodynamic stability of the gravastar was also discussed. Later, the Mazur and Mottola research was generalised and the stability of the star was tested by Visser and Wiltshire [3] by taking the physical properties and state equation. The gravastar solutions with anisotropic pressure and with various realistic backgrounds are presented by DeBenedictis *et al* [4]. They also investigated the requirements of equilibrium energy and developed the polytropic state equation. The reliability of a gravastar against the general disruption was shown by Chirenti and Rezzolla [5]. The concept that the gravastar’s optical images have an unstable circular orbit was analysed by Sakai *et al* [6]. In

reality, they believed and identified two optical sources in depth.

The Big Bang theory is the fundamental theory to explain the birth of the Universe. This theory claimed that the Universe as we know has started with a little singularity, then expanded exponentially over the next 14 billion years to the cosmos that we are familiar with today. General relativity (GR) has been found to be a very interesting and captivating theory for the better understanding of many cosmic puzzles. This theory may have to be modified to explain the large-scale structures, the cosmic expansion of the Universe and the massive objects at the quantum level. Therefore, the concept of modified theories of gravity was introduced. In this direction, $f(R)$ theories were introduced. In these theories, the Ricci scalar in the action function was replaced by its generic function so that the higher-order invariants could be involved. Additionally, $f(R)$ theories depict how the geometry is linked with matter through non-minimal coupling. Fay *et al* [7] tried to identify different $f(R)$ functions. To achieve this, they have presumed the cosmic history and matter or radiation dominant in their respective eras. Poplawski [8] constructed a $\Lambda(T)$ model. The main aim of his model is that we do not have to transform from one metric to the next (conformal) and no one challenges the metric because we use the same metric tensor, which is physical. Afterwards, to figure out the quantum effects or the exotic imperfect fluids and for the arbitrarily matter–geometry coupling that is not minimal, the generalisation in the $f(R)$ theories has been established. Harko *et al* [9] designated the $f(R, T)$ theory in which T represents the energy–momentum tensor trace. They described numerous forms of $f(R, T)$ and their respective field equations to study the scalar field model. Das *et al* [10] explored the important features of gravastar in $f(T)$ gravity and evaluated its three regions. Moreover, Debnath [11] evaluated the different physical features of charged gravastar in the $f(T)$ gravity.

In $f(R, T)$ theory if we use $T = 0$ then the theory will reduce to $f(R)$ and the effects of T would vanish. This insists the further generalisation of $f(R, T)$ theory which encouraged matter–geometry coupling that is strong but non-minimal. Haghani *et al* [12] brought out the $f(R, T, Q)$ theory ($Q \equiv R_{\mu\nu}T^{\mu\nu}$) which associates the Ricci scalar and the stress energy–momentum tensor contraction. In the case of both conservative and non-conservative situations, the field equations are extracted for the test particle motion. Also, Dolgov–Kawasaki instability along with the stability condition

and a few cosmological problems were examined. The $f(R, T, Q)$ phenomenology was explained and the fluctuations in that gravity was examined by Odintsov and Sáez-Gómez [13]. To address stability in terms of power-law as well as de-Sitter solution, Baffou *et al* [14] investigated a $f(R, T, R_{\mu\nu}T^{\mu\nu})$ gravity model. Ayuso *et al* [15] conferred a widespread framework in $f(R, T, Q)$ theory and demonstrated that the conformal and non-minimal relations to the fields lead typically to higher-order equations. Yousaf *et al* [16] measured the complexity in $f(R, T, Q)$ gravity for the charged static spherical system. Yousaf *et al* [17] introduced the new definition of complexity under the consideration of cylindrically symmetric metric in the $f(R, T, Q)$ gravity. They have also done this work for the charged celestial bodies [18]. The reason to work in this modified theory has been explained in Yousaf *et al* [19–22].

Ghosh *et al* examined the gravastar-like structures in higher-dimensional space–time, in (3+1) dimensions with Karmarkar condition and Kuchowicz matrix potential. Moreover, their realistic features are depicted graphically as well as mathematically along with the formulation of three regions independently in [23–26]. Bhatti *et al* [27] constructed a thin-shell gravastar model and discussed its physically acceptable characteristics in the context of non-commutative geometry. Das *et al* [28] discussed the realistic features of the gravastar graphically and mathematically along with its different regions in the $f(R, T)$ gravity. Sengupta *et al* [29] investigated the gravastar model in the background of Randall–Sandrum (RS) brane gravity. They have also computed the surface red-shift to visualise gravastar’s stability within RS brane gravity. Ray *et al* [30] gave a detailed overview of the gravastar-like structures poring over different modified theories. They also portrayed the astrophysical observational possibilities of gravastar-like structures in the future.

This motivates us to construct a model of the gravastar which is cylindrically symmetric about its axis, having the effective matter and isotropic pressure, in this theory. The structure of our work in the $f(R, T, Q)$ theory is the effective matter which is defined using the variational principle and Einstein Hilbert action in §2. The modified field and non-conservation equations are evaluated along with hydrostatic equilibrium condition. We also performed mathematical calculation of each region separately in §3. The junction conditions, surface stress-energy and surface pressure are determined in §4. Some models’ physical characteristics are explained with the help of their graphical representations in §5. In §6 we give our conclusion.

2. Basic mathematical formalism of the $f(R, T, Q)$ theory

In $f(R, T, Q)$ theory [12] the Hilbert action is designated as

$$S = \frac{1}{2} \int d^4x f(R, T, R_{\alpha\beta} T^{\alpha\beta}) \sqrt{-g} + \int d^4x L_m \sqrt{-g}, \tag{1}$$

where T, R indicate the trace of energy–momentum tensor and the Ricci scalar, while $Q \equiv R_{\alpha\beta} T^{\alpha\beta}$. L_m is the matter Lagrangian and g is the magnitude of the metric tensor. By giving variations of the above action integral with metric tensor, we have

$$\begin{aligned} & -G_{\alpha\beta}(-f_R + f_Q L_m) - g_{\alpha\beta} \\ & \times \left\{ -\frac{R}{2} f_R + \frac{f}{2} - \square f_R - \frac{1}{2} \nabla_a \nabla_b (f_Q T^{ab}) - L_m f_T \right\} \\ & + 2f_Q R_{b(\alpha} T_{\beta)}^b + \frac{1}{2} \square (f_Q T_{\alpha\beta}) \\ & - \nabla_\pi \nabla_\alpha [T_{\beta} f_Q] - 2(f_T g^{\pi\rho} + f_Q R^{\pi\rho}) \frac{\partial^2 L_m}{\partial g^{\alpha\beta} \partial g^{\pi\rho}} \\ & - T_{\alpha\beta}^{(m)} \left(f_T + 1 + \frac{R}{2} f_Q \right) - \nabla_\alpha \nabla_\beta f_R = 0, \tag{2} \end{aligned}$$

where $\square = g^{\alpha\beta} \nabla_\alpha \nabla_\beta$, ∇_α is a covariant derivative, subscripts R, T, Q describe the partial differentiation with respect to R, T, Q , respectively. We can write it alternatively as

$$G_\nu^\mu = T_\nu^{\mu(\text{eff})}, \tag{3}$$

where

$$\begin{aligned} T_{ab}^{(\text{eff})} = & \frac{1}{f_R - L_m f_Q} \\ & \times \left[\left(f_T + \frac{1}{2} R f_Q + 1 \right) T_{ab}^{(m)} + \left\{ \frac{f}{2} - \frac{f_R R}{2} \right. \right. \\ & \left. \left. - L_m f_T - \frac{1}{2} \nabla_c \nabla_d (f_Q T^{cd}) \right\} g_{ab} \right. \\ & \left. - \frac{1}{2} \square (f_Q T_{ab}) - (g_{ab} g^{cd} \nabla_c \nabla_d - \nabla_a \nabla_b) f_R \right. \\ & \left. - 2f_Q R_{c(a} T_{b)}^c + \nabla_c \nabla_{(a} [T_{b)}^\alpha f_Q] \right. \\ & \left. + 2(f_Q R^{cd} + f_T g^{cd}) \frac{\partial^2 L_m}{\partial g^{ab} \partial g^{cd}} \right] \tag{4} \end{aligned}$$

can be regarded as the effective energy–momentum tensor. The purpose of this study is to construct the locally isotropic gravastars. Therefore, we assume the usual energy–momentum tensor as

$$T_{\mu\nu}^{(m)} = (\rho + P)u_\mu u_\nu - P g_{\mu\nu},$$

where μ, P are the energy density and pressure of the fluid, while u_μ is the fluid four-velocity. Now, the trace of eq. (2), turns out to be

$$\begin{aligned} & 3\square f_R + \frac{1}{2}\square(Tf_Q) - (f_T + 1)T \\ & + \nabla_\pi \nabla_\rho (f_Q T^{\alpha\beta}) + R \left(-\frac{T}{2} f_Q + f_R \right) \\ & + (4f_T + Rf_Q)L_m - 2f + 2R_{\alpha\beta} T^{\alpha\beta} f_Q \\ & - 2\frac{\partial^2 L_m}{\partial g^{\gamma\delta} \partial g^{\pi\rho}} (f_T g^{\alpha\beta} + f_Q R^{\alpha\beta}). \end{aligned}$$

One can notice that this trace is entirely different from that of GR. It is because of the inclusion $f(R, T, Q)$ corrections in the action function.

3. Formation of cylindrical gravastars in $f(R, T, Q)$ gravity

We consider a cylindrical space–time to construct the three-layered gravastar model as

$$ds^2 = -H(r)dt^2 + K(r)dr^2 + r^2(d\phi^2 + \alpha^2 dz^2), \tag{5}$$

where

$$H(r) = \sqrt{\alpha^2 r^2 - \frac{4M}{r}}$$

and

$$K(r) = \frac{1}{H(r)}.$$

The parameter α is treated as a constant with dimension L^{-1} . The static, cylindrically symmetric vacuum solutions were found in the early 20th century by Weyl and Levi-Civita. They were interested in the more general problem of static geometries that depend on z as well as r . Levi-Civita proposed the vacuum static solution to analyse the cylindrical symmetric matter configurations that prompted the researchers to unveil the mysteries of the astrophysical objects. Cylindrical symmetry (combining translation along and rotation around an axis) has empirically relevant repercussions in the classical as well as quantum physics. The intuitive idea of extending the symmetries from spherical to the cylindrical is very clear due to the fact that it is useful in obtaining significant information about the self-gravitating fluids. Furthermore, various physical features of these fluids play vital roles in the evolution and the dynamical instabilities of self-gravitating systems. The corresponding Einstein tensors are found as follows:

$$G_0^0 = \frac{-K'}{rK^2} + \frac{1}{r^2K}, \tag{6}$$

$$G_1^1 = \frac{H'}{KHr} + \frac{1}{Kr^2}, \tag{7}$$

$$G_3^3 = \alpha^2 G_2^2 = \frac{-1}{4} \left[\frac{K'H'}{HK^2} - \frac{2H''}{KH} + \frac{H'^2}{KH^2} + \frac{2K'}{rK^2} - \frac{2H'}{K Hr} \right], \tag{8}$$

where prime denotes the derivative corresponding to the radial coordinate r . Then the complete equations of motion for $f(R, T, Q)$ gravity can be calculated by eqs (3) and (6)–(8) as

$$-\frac{K'}{rK^2} + \frac{1}{r^2K} = \frac{-8\pi}{f_R + \rho f_Q} \times \left[\rho\delta_1 + \rho'\delta_2 + P\delta_3 + P'\delta_4 + \frac{P''f_Q}{2K} + D_6 \right], \tag{9}$$

$$\frac{H'}{K Hr} + \frac{1}{K r^2} = \frac{8\pi}{f_R + \rho f_Q} \times \left[\rho\delta_5 + \frac{\rho'f_Q H'}{4HK} + P\delta_6 + P'\delta_7 - \frac{P''f_Q}{K} + D_7 \right], \tag{10}$$

$$-\frac{1}{4} \left[\frac{K'H'}{HK^2} - \frac{2H''}{KH} + \frac{H'^2}{KH^2} + \frac{2K'}{rK^2} - \frac{2H'}{K Hr} \right] = \frac{8\pi}{f_R + \rho f_Q} \left[\rho\delta_8 - \frac{\rho'H'f_Q}{4HK} + P\delta_9 + P'\delta_{10} - \frac{P''f_Q}{2K} + D_8 \right]. \tag{11}$$

The values of δ_i 's where $i = 1-10$ and that of D_j 's where $j = 6, 7, 8$ are given in Appendix. The terms D_6, D_7 and D_8 represent the effects of the dark source.

In this theory, the divergence of effective energy-momentum tensor is non-zero, thus indicating that our theory is non-conserved in nature. This would allow the test particles to allow the non-geodesic motion. Thus, the corresponding equation is calculated as

$$\frac{\partial P^{\text{eff}}}{\partial r} + \frac{H'}{2H(r)}[\rho^{\text{eff}} + P^{\text{eff}}] - ZK(r) = 0, \tag{12}$$

where Z is given in Appendix. Using eq. (9), we obtain

$$K^{-1}(r) = \frac{1}{2} - \frac{2m}{\alpha r} + \frac{8\pi}{r} \int \rho^{*(\text{eff})} r^2 dr, \tag{13}$$

where m is the mass of the sphere. Equation for the hydrostatic equilibrium condition in the $f(R, T, Q)$ theory can be obtained by working on eqs (10), (12), (13). This equation helps us to understand the problem of stability

$$\frac{\partial P^{\text{(eff)}}}{\partial r} - \frac{Z}{\frac{1}{2} - \frac{2m}{\alpha r} + \frac{8\pi}{r} \int \rho^{*(\text{eff})} r^2 dr} + \left[\frac{8\pi}{(f_R + \rho f_Q) \left(\frac{1}{2} - \frac{2m}{\alpha r} + \frac{8\pi}{r} \int \rho^{*(\text{eff})} r^2 dr \right)} \right]$$

$$\times \left(\rho\delta_5 + \frac{\rho'f_Q H'}{4H(r)K(r)} + P\delta_6 + P'\delta_7 - P''f_Q \left(\frac{1}{2} - \frac{2m}{\alpha r} + \frac{8\pi}{r} \int \rho^{*(\text{eff})} r^2 dr \right) + D_7 \right) - \frac{\frac{1}{2} - \frac{2m}{\alpha r} + \frac{8\pi}{r} \int \rho^{*(\text{eff})} r^2 dr}{r^2} \left[\frac{(\rho^{\text{(eff)}} + P^{\text{(eff)})}}{\frac{2}{r} + \frac{4\pi\rho'f_Q}{f_R + \rho f_Q}} \right] = 0. \tag{14}$$

Now, we shall study the structure of gravastar in $f(R, T, Q)$ gravity. For this purpose, we model three different regions of the celestial body one by one.

3.1 Region I

This is the region which is responsible for making the hypothetical star singularity-free, i.e., all the mass would not be able to gather at one point. This portion is assumed to be filled with dark energy, and due to this, it would apply the repulsive force on the shell. The information about the dark energy is gathered through the cosmological constant as it is found to be the best candidate in recognising it. The barotropic EoS for this region is

$$P = -\rho. \tag{15}$$

This is a well-known barotropic EoS with $\omega = -1$, which shows the presence of vacuum energy in this region. One can call it the dark energy EoS. With this EoS, the energy density become constant. Then

$$\rho = \rho_0(\text{constant}). \tag{16}$$

Thus, pressure turns out to be

$$P = -\rho_0. \tag{17}$$

Substituting eq. (17) in (9) we have the value of $1/K(r)$ as

$$K^{-1}(r) = -\frac{1}{r} \int \left[\frac{8\pi r^2}{f_R + \rho_0 f_Q} (\rho_0(\delta_1 - \delta_3) + D_6) \right] dr + \frac{A}{r}. \tag{18}$$

To obtain a regular solution, the integration constant A must be zero.

$$K^{-1}(r) = a(r), \tag{19}$$

where

$$a(r) = -\frac{1}{r} \int \left[\frac{8\pi r^2}{f_R + \rho_0 f_Q} (\rho_0(\delta_1 - \delta_8) + D_6) \right] dr.$$

Now, the value of H for the interior region is

$$H(r) = BK^{-1}(r) + e^{b(r)}, \tag{20}$$

where

$$b(r) = \int \left[\frac{8\pi Kr}{f_R + \rho_0 f_Q} (\rho_0(\delta_1 - \delta_3 + \delta_5 - \delta_6) + D_6 + D_7) \right] dr.$$

B denotes the integration constant. The gravitational mass is evaluated as

$$M(D) = \int_0^D \left[\frac{4}{3} \pi \alpha \rho_0^{(\text{eff})} r^2 + \frac{\alpha}{8} \right] dr = \frac{4}{3} \pi \alpha \rho_0^{(\text{eff})} D^3 + \frac{\alpha D}{8}. \tag{21}$$

This function includes the correction terms due to the modified gravity in the matter content of the cylindrical gravastar-like bodies.

3.2 Region II

The shell is constituted of effective matter including ultrarelativistic fluid and the isotropic pressure in contrast to the internal region of dark energy. We reduced the shell into one layer of thickness rather than the three layers of thin shell assembled with different suppositions as proposed by Mazur and Mottola. The relevant EoS for the shell is $\rho = P$. The shell's thickness is treated to be extremely thin, i.e., the range of $K^{-1}(r)$ lies between zero and one. Such assumptions always make equations smooth to handle our calculations [31]. In addition, this kind of fluid explores primarily the cosmological and astrophysical processes [32–36]. Using $P = \rho$, the first two field equations give

$$\frac{d}{dr}(K^{-1}(r)) = \gamma_0(r), \tag{22}$$

where

$$\gamma_0(r) = \frac{8\pi r}{f_R + \rho f_Q} \left[\rho(\delta_5 + \delta_6 - \delta_1 - \delta_3) + \rho' \left(\delta_7 - \delta_4 - \frac{H' f_Q}{4H(r)K(r)} - \delta_2 \right) - \frac{\rho'' 3f_Q}{2K(r)} - D_6 + D_7 \right].$$

Furthermore, by using the first and last field equations and $P = \rho$, we get

$$\left[\frac{H'}{4H(r)} + \frac{3}{r} \right] \frac{d}{dr}(K^{-1}(r)) = \gamma_1(r), \tag{23}$$

where

$$\gamma_1(r) = \frac{8\pi}{f_R + \rho f_Q} \left[\rho(\delta_8 + \delta_9 - \delta_1 - \delta_3) \right.$$

$$\left. + \rho' \left(\delta_{10} - \delta_2 - \frac{H' f_Q}{4H(r)K(r)} - \delta_4 \right) - \frac{\rho'' f_Q}{K(r)} + D_8 - D_6 \right].$$

Integrating eq. (22) we have

$$K^{-1}(r) = \int \gamma_0(r) dr + C, \tag{24}$$

where C denotes the integration constant. The variation of radius r is from D to $D + \epsilon$. If $\epsilon < 1$, in such a scenario we obtain $C < 1$ which gives $K^{-1}(r) \ll 1$. Equating eqs (22) and (23) we determine

$$H(r) = e^{4 \int \frac{\gamma_1(r)}{\gamma_0(r)} dr} + Fr^{-12}, \tag{25}$$

where F is the constant of integration. Solving eq. (12) we get

$$\rho^{(\text{eff})} = P^{(\text{eff})} = \frac{1}{H(r)} \left[\int Z dr + h \right], \tag{26}$$

where h is the constant of integration. The value of Z under the consideration of the EoS of the shell, i.e., $P = \rho$ is described as

$$Z = \frac{2}{2 + Rf_Q + 2f_T} \left[\frac{f'_Q PK'H'}{4K^2 H} - \frac{f'_Q PH''}{2HK} + \frac{f'_Q PH'^2}{4KH^2} + \frac{f'_Q PK'}{rK^2} + \frac{f_Q PK''H'}{4HK^2} + \frac{3f_Q PK'H''}{4HK^2} - \frac{f_Q PH'''}{2HK} + \frac{f_Q PH''H'}{4H^2 K} - \frac{f_Q PH^3}{2KH^3} - \frac{f_Q PK''}{rK^2} - \frac{f_Q PK'}{r^2 K^2} - \frac{f_Q PK'^2 H'}{2HK^3} + \frac{f_Q P'K'H'}{4K^2 H} - \frac{f_Q P'H''}{2KH} + \frac{f_Q P'H'^2}{4KH^2} - 2P'f_T - 2Pf'_T + \frac{2f_Q P'}{r^2 K} + \frac{f'_Q PH'}{KHr} + \frac{f'_Q P}{Kr^2} + \frac{f_Q P'H'}{KHr} - \frac{f_Q R'P}{2} - \frac{f'_Q RP}{2} \right].$$

Figure 1 is a graph plotted between the radius and the density which reassure us that the EoS adopted for the thin shell of the gravastar is accurate as it indicates the direct relation between energy density and pressure.

3.3 Region III

The exterior area of the de-Sitter is vacuumed, with the state equation $\rho = P = 0$. The suitable exterior metric

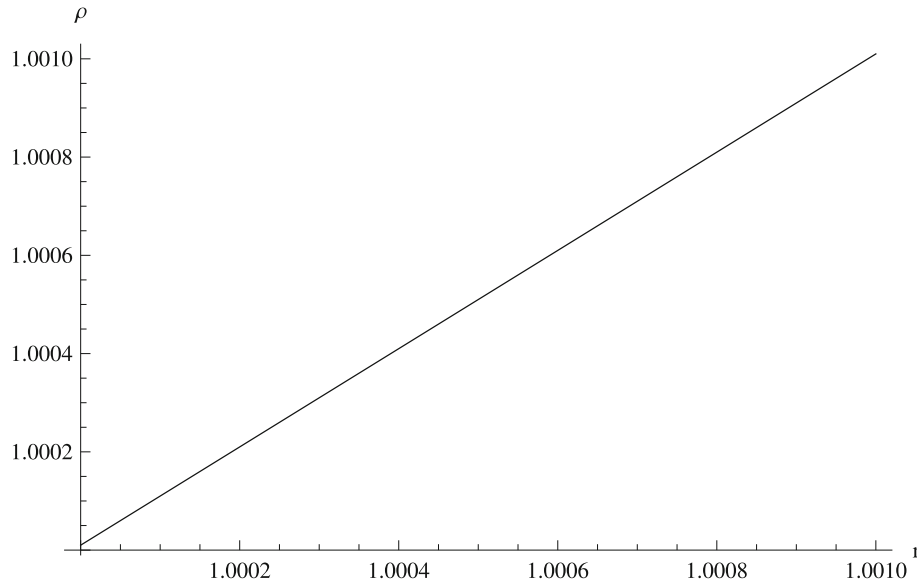


Figure 1. Plot showing the density–radius relationship.

in this case can be taken as follows:

$$ds^2 = - \left(1 - \frac{r^2}{\beta^2}\right) dt^2 + \left(1 - \frac{r^2}{\beta^2}\right)^{-1} dr^2 + r^2(d\phi^2 + \alpha^2 dz^2), \quad (27)$$

where β is a constant.

4. Junction conditions

Junction conditions connect the interior and exterior space–time of any self-gravitating object precisely at the hypersurface. These conditions have accomplished noteworthy significance in studying the behaviour of the thin shell, boundaries of gravitational as well as astronomical objects. The thin shell formalism of Darmois–Israel [37,38] formulates the requirements for the smooth connection of the metrics to the surface. Continuous metric coefficients are needed in this formalism at the junction of $r = D$ between two regions. It is possible that they do not have any continuous derivatives. The stress–energy tensor S_j^i can also be determined using the formalism discussed above. To match region III with I at the hypersurface, Yousaf *et al* [39] evaluated the junction conditions in the $f(R, T, Q)$ theory. The fulfillment of the equations mentioned in it is needed for the sake of R and Q continuity in a thin shell. Lanczos equation [40–43] used to evaluate the intrinsic surface stress–energy tensor is written as follows:

$$S_j^i = -\frac{1}{8\pi}(\kappa_j^i - \delta_j^i \kappa_k^k). \quad (28)$$

The discontinuity in extrinsic curvatures arises due to $\kappa_j^i = K_{ij}^+ - K_{ij}^-$. The + sign signifies region I and the – one indicates region III. The second fundamental forms, which are connected to both sides of the shell, are as follows:

$$K_{de}^+ = -n_c^+ \left[\frac{\partial^2 x_c}{\partial \xi^d \partial \xi^e} + \Gamma_{ab}^c \frac{\partial x^a}{\partial \xi^d} \frac{\partial x^b}{\partial \xi^e} \right] \Big|_{\Sigma}, \quad (29)$$

where the intrinsic coordinates on the shell and the unit normal to the surface Σ are described by ξ^d and n_c^+ respectively.

$$ds^2 = f(r)dt^2 - \frac{dr^2}{f(r)} - r^2(d\theta^2 + \sin^2 \theta d\phi^2) \quad (30)$$

and for this kind of metric, n_c^+ is specified as

$$n_c^+ = \pm \left| g^{ab} \frac{\partial f}{\partial x^a} \frac{\partial f}{\partial x^b} \right|^{-1/2} \frac{\partial f}{\partial x^c} \quad (31)$$

with $n^a n_a = 1$. The stress–energy tensor $S_j^i = \text{diag}[\sigma, -\nu, -\nu, -\nu]$ can be determined utilising the Lanczos equations, where surface energy density is σ and surface pressure is ν . The surface energy density is formulated as

$$\sigma = \frac{-1}{4\pi D} [\sqrt{f}]_{-}^{+}. \quad (32)$$

Putting the values in the above equation we obtain the surface stress energy density as

$$\sigma = \frac{-1}{4\pi D} \left[\sqrt{1 - \frac{D^2}{\beta^2}} - \sqrt{a(D)} \right]. \quad (33)$$

The value of $a(D)$ will be obtained by putting $r = D$ in $a(r)$. The surface pressure is formulated as

$$v = \frac{-\sigma}{2} + \frac{1}{16\pi} \left[\frac{f'}{\sqrt{f}} \right]_+^- \tag{34}$$

Substituting values in the formula we get

$$v = \frac{1}{8\pi D} \left[\frac{1 - \frac{2D^2}{\beta^2}}{\sqrt{1 - \frac{D^2}{\beta^2}}} - \frac{a(D) + \frac{Da'(D)}{2}}{\sqrt{a(D)}} \right], \tag{35}$$

where

$$a(D) = -\frac{1}{D} \int \left[\frac{8\pi D^2}{f_R + \rho_0 f_Q} (\rho_0(\delta_1 - \delta_8) + D_6) \right] dr.$$

The formula to calculate the mass of the thin shell of the gravastar is

$$m_s = 4\pi D^2 \sigma. \tag{36}$$

By substituting the value of surface energy density, we have

$$m_s = D \left[\sqrt{a(D)} - \sqrt{1 - \frac{D^2}{\beta^2}} \right]. \tag{37}$$

5. Physical features of the model

This portion is assigned to discuss physical properties like length, energy, entropy and EoS of the stellar objects mathematically and graphically.

5.1 Shell's proper length

As described earlier, the thickness of the shell of the gravastar is presumed to be extremely thin, i.e., $\epsilon \ll 1$. The length of the shell is related to the thickness of the shell. We can calculate the length from the surface $r = D$ to $r = D + \epsilon$ using the following equation:

$$l = \int_D^{D+\epsilon} \sqrt{K(r)} dr = \int_D^{D+\epsilon} \frac{dr}{\sqrt{\int \gamma_0(r) dr + C}}. \tag{38}$$

Figure 2 which is a plot between the length and the thickness of the shell, demonstrates the direct relationship between them.

5.2 Energy content

Region I of the gravastar is responsible for producing the energy, having EoS $\rho = -P$. This energy is found to be repulsive in nature. However, the energy within

the shell is given as

$$\begin{aligned} \epsilon &= \int_D^{D+\epsilon} 4\pi \rho^{(\text{eff})} r^2 dr \\ &= 4\pi \int_D^{D+\epsilon} \left[\frac{r^2}{H(r)} \left(\int Z(r) dr + h \right) \right] dr. \end{aligned} \tag{39}$$

Figure 3 shows that for a constant thickness, the value of the energy changes or it might have any value.

5.3 Entropy

Entropy is a property of a system's equilibrium states from the perspective of thermodynamics. Macroscopic variables like strain, temperature and density are described by these states. The density of entropy is inversely related to the cube of the scale factor. The scale factor indicates the expansion of the Universe. So, the entropy density is found to be negligible in the inner region and we can roughly say that region I constitutes zero entropy density. The entropy within the shell is evaluated as

$$S = \int_D^{D+\epsilon} 4\pi s(r) r^2 \sqrt{K(r)} dr. \tag{40}$$

The entropy density is represented by $s(r)$. Entropy density is formulated as

$$s(r) = \frac{\alpha^2 k_B^2 T(r)}{4\pi \hbar^2} = \alpha \left(\frac{k_B}{\hbar} \right) \sqrt{\frac{p^{(\text{eff})}}{2\pi}}, \tag{41}$$

where α denotes a constant with no dimension. Planckian units are $k_B = \hbar = 1$ and the geometric units are $G = c = 1$. The entropy density comes out to be

$$s(r) = \alpha \sqrt{\frac{p^{(\text{eff})}}{2\pi}}. \tag{42}$$

Putting the value of entropy density in eq. (40), the entropy comes out to be

$$\begin{aligned} S &= \frac{4\pi \alpha}{\sqrt{2\pi}} \\ &\times \int_D^{D+\epsilon} \left[\sqrt{\frac{\int Z dr + h}{H(r)}} \left(\frac{r^2}{\sqrt{\int \gamma_0(r) dr + C}} \right) \right] dr. \end{aligned} \tag{43}$$

Figure 4 shows that the entropy of the shell of the gravastar shows persistent relationship with the thickness of the shell of the gravastar.

5.4 Equation of state

The state equation has a vital role in determining the system's behaviour and in knowing its future. It connects

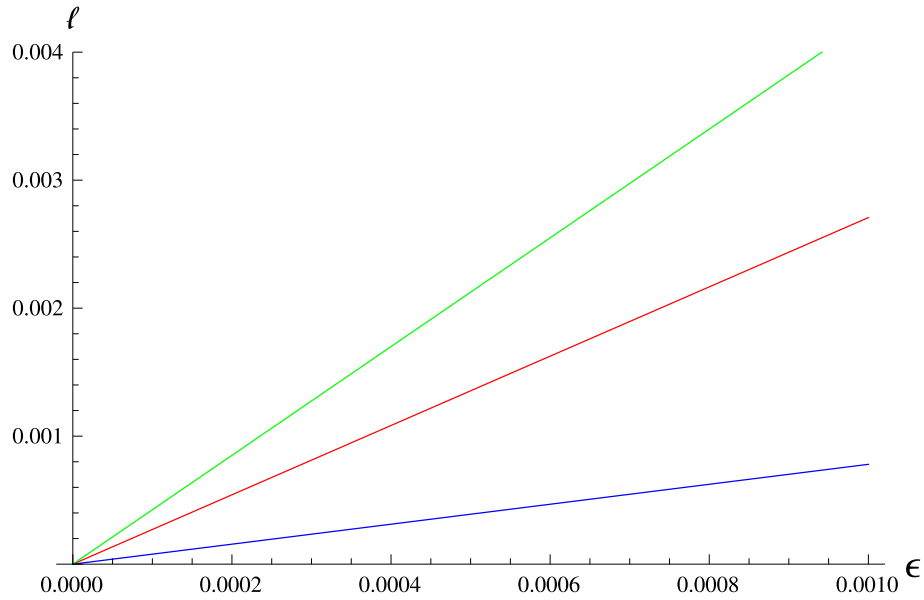


Figure 2. Plots of proper length vs. the thickness of the shell.

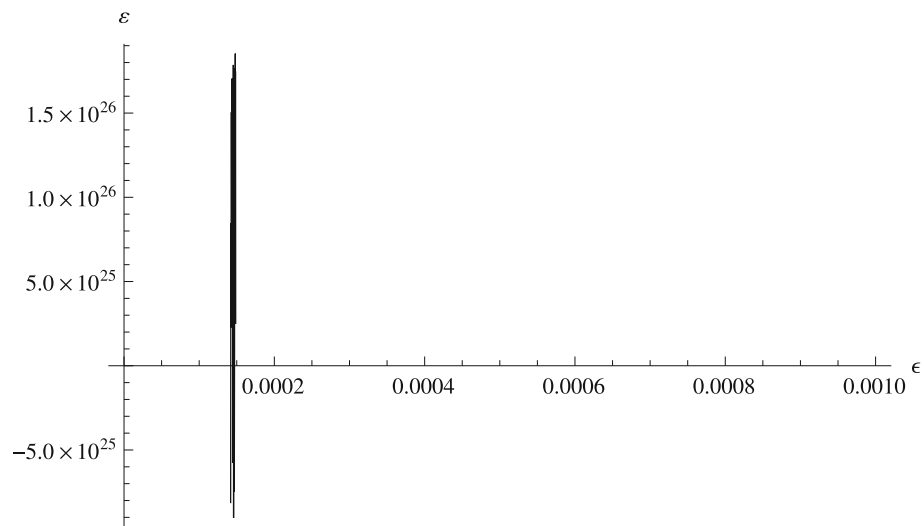


Figure 3. Plot of energy vs. thickness of the shell.

the state variables that allow us to illustrate the system’s physical aspects. Within our system, surface density and surface pressure are the state variables. So, at $r = D$ the EoS can be described as

$$v = \omega(D)\sigma. \tag{44}$$

$$\omega(D) = \frac{\left[\frac{1 - \frac{2D^2}{\beta^2}}{\sqrt{1 - \frac{D^2}{\beta^2}}} - \frac{a(D) + \frac{Da'(D)}{2}}{\sqrt{a(D)}} \right]}{2 \left[\sqrt{a(D)} - \sqrt{1 - \frac{D^2}{\beta^2}} \right]}. \tag{45}$$

To get the real value of $\omega(D)$, both $1 - (D^2/\beta^2)$ and $a(D)$ should be chosen equal to 1 or greater than 1. Then applying the binomial series upto the first order

on the above equation, we obtain the approximate value of $\omega(D)$.

$$\omega(D) \approx \frac{\left[1 - \frac{3D^2}{2\beta^2} - \frac{2a(D) - Da'(D)}{2\sqrt{a(D)}} \right]}{2 \left[\frac{D^2}{\beta^2} - 1 + \sqrt{a(D)} \right]}. \tag{46}$$

$\omega(D)$ will have positive value if the value chosen for

$$\frac{3D^2}{2\beta^2} - \frac{2a(D) - Da'(D)}{2\sqrt{a(D)}} < 1$$

and

$$\frac{D^2}{\beta^2} + \sqrt{a(D)} - 1 > 1.$$

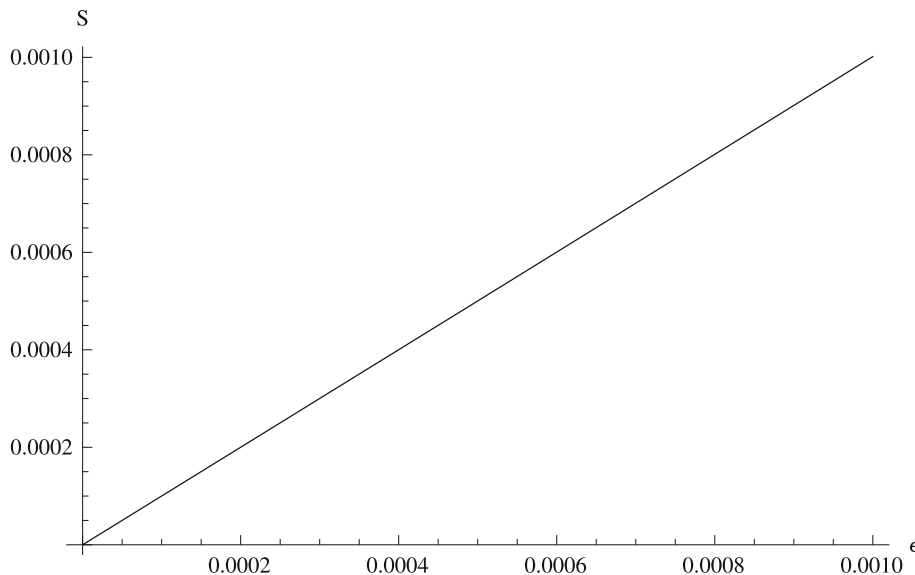


Figure 4. Plot showing the relationship between entropy and thickness of the shell.

The value of $\omega(D)$ will be negative if any one of the fractions

$$\left(1 - \frac{3D^2}{2\beta^2} - \frac{2a(D) - Da'(D)}{2\sqrt{a(D)}}, \frac{D^2}{\beta^2} + \sqrt{a(D)} \right) < 1.$$

The real value will only be attained if $a(D)$ is positive and greater than 1. The positive and negative values of $\omega(D)$ may provide a powerful medium to construct the model for the thin shell of gravastars. These conditions may be beneficial for recognising the numerical simulation of cylindrical isotropic gravastar.

6. Conclusion

This article explores the impact of $f(R, T, Q)$ theory on the formation of relativistic isotropic cylindrical gravastars. The gravastar structure is known to be an alternate image of the black hole. For this purpose, we assume an appropriate static metric (that is cylindrically symmetric about its own axis) to examine the gravastar. Its metric coefficients were then derived separately for the three regions. The physical properties successively try to enlighten significant results. The surface outside the boundary was taken as a vacuum. We have taken the space–time mentioned in eq. (27) into account for this purpose and performed matching through Israel and Darmois conditions. We then computed a collection of accurate and regular models of the collapsing star that could facilitate physically depicting the reasonable prospects of gravastar in the $f(R, T, Q)$ theory. They are specified as follows:

- (1) *Description of pressure and density:* To investigate the physics between the radius and the energy density in the presence of effective matter and under the consideration of the $f(R, T, Q)$ theory, we considered the arbitrary function of $Z(r)$, by taking $\alpha = 1$ and $M = 4.2 \times 10^{27}$. From figure 1 we found that there exists a direct relationship between the radius and the density. Along with this, the density is directly proportional to the pressure in $f(R, T, Q)$ theory.
- (2) *Proper length:* We have analysed the role of the proper length with regard to shell thickness, which involves the effective matter in the presence of modified $f(R, T, Q)$ theory. Figure 2 depicts that the shell’s length increases with its thickness.
- (3) *Energy:* Figure 3 shows the energy variance in relation with shell thickness under the influence of $f(R, T, Q)$ terms. This graph demonstrates that at a certain value of the thickness the value obtained for the energy will be different.
- (4) *Entropy:* Figure 4 shows the direct relationship between the thickness and the entropy of the shell.
- (5) *Equation of state:* $\omega(D)$ will have positive value if

$$\frac{3D^2}{2\beta^2} - \frac{2a(D) - Da'(D)}{2\sqrt{a(D)}} < 1$$

and

$$\frac{D^2}{\beta^2} + \sqrt{a(D) - 1} > 1.$$

The value of $\omega(D)$ will be negative if any one of the fractions

$$\left(1 - \frac{3D^2}{2\beta^2} - \frac{2a(D) - Da'(D)}{2\sqrt{a(D)}}, \frac{D^2}{\beta^2} + \sqrt{a(D)}\right) < 1.$$

The real value will only be attained if $a(D)$ is positive and greater than 1.

We have not transformed our results from cylindrical symmetry to the spherical one. However, we can compare our results with the spherical one [20]. Firstly, for the similar range of radius [1, 1.0010], the range of density lies in [1, 1.2008×10^{-6}] for spherical space-time whereas this regions is found to be [1, 1.0010], in the case of cylindrical space-time. This shows that for the same range of radius, the shell is more dense for the cylindrical space-time. Secondly, for spherical space-time the maximum length of the shell of the gravastar was 0.0020 for $0 < \epsilon < 0.0010$ while in the present work it is 0.0040. This means that the length is increased in our scenario for the same thickness as in the spherical case. Next, in cylindrical space-time, for the constant thickness of 0.0002, we have varied the values of the energy but in spherical case it has the relation of direct proportionality. Finally, the amount of entropy is increased in our work (i.e., 0.0010) compared to the spherical one (i.e., 5×10^{-6}) with the small variations in the thickness of the shell of the gravastar.

Appendix

The values of δ_i 's where $i = 1-10$ and that of D_j 's where $j = 6,7,8$ appeared in eqs (9), (10) and (11) are discussed as follows:

$$\begin{aligned} \delta_1 &= 1 + \frac{Rf_Q}{2} - \frac{9f_QH'^2}{8KH^2} - \frac{2f_Q}{r^2K} \\ &\quad - \frac{K'H'f_Q}{4HK^2} + \frac{f'_QH'}{4H^2} + \frac{3f_QH''}{4KH} - \frac{f''_Q}{2K} \\ &\quad - \frac{3f'_QH'}{4KH} + \frac{K'f'_Q}{4K^2} + \frac{5f_QH'}{4rKH}, \\ \delta_2 &= \frac{K'f_Q}{4K^2} - \frac{f'_Q}{K} - \frac{f_QH'}{2H^2}, \\ \delta_3 &= -\frac{5H'^2f_Q}{8KH^2} - \frac{f''_Q}{K} - \frac{f'_QK'}{4K^2} \\ &\quad - \frac{f_QH''}{4KH} + \frac{f'_Q}{2rK} - \frac{3f_QH'}{4rKH} \\ &\quad - \frac{f'_Q}{rKH} - \frac{2f'_Q}{rH} - \frac{f_Q}{r^2KH}, \end{aligned}$$

$$\begin{aligned} \delta_4 &= \frac{f'_Q}{K} - \frac{f_QK'}{4K^2} + \frac{f_Q}{2rK}, \\ D_6 &= -\frac{f}{2} + \frac{f_RR}{2}, \\ \delta_5 &= f_T - \frac{f'_QH'}{4H^2} - \frac{f_QK'H'}{4HK^2} \\ &\quad - \frac{H''f_Q}{4KH} - \frac{f_QH'^2}{8KH^2} + \frac{2f_Q}{Kr^2} \\ &\quad - \frac{f_QH'}{4rHK} + \frac{f'_QH'}{2HK}, \\ \delta_6 &= f_T + \frac{Rf_Q}{2} + 1 - \frac{f'_QH'}{4KH} \\ &\quad + \frac{2f''_Q}{K} - \frac{5H'^2f_Q}{8KH^2} - \frac{f_QH'}{4rKH} - \frac{f_QK''}{2K^2} \\ &\quad - \frac{3f_QH''}{4HK} - \frac{H'K'f_Q}{4HK^2} - \frac{3f'_Q}{2rK} - \frac{4K'f_Q}{rK^2}, \\ \delta_7 &= \frac{f'_Q}{K} - \frac{3f_Q}{2rK} - \frac{f_QH'}{4HK}, \\ D_7 &= \frac{f}{2} - \frac{Rf_R}{2} - \frac{H'f'_R}{2HK} - \frac{2f'_R}{rK}, \\ \delta_8 &= f_T - \frac{f'_QH'}{4H^2} - \frac{H'^2f_Q}{8KH^2} - \frac{H''f_Q}{4HK} \\ &\quad + \frac{K'H'f_Q}{4HK^2} + \frac{2f_Q}{Kr^2} - \frac{f_QH'}{4HKr}, \\ \delta_9 &= f_T + \frac{Rf_Q}{2} + 1 - \frac{3f'_QH'}{4HK} \\ &\quad - \frac{f_QH'^2}{8KH^2} + \frac{f''_Q}{2K} + \frac{3f'_QK'}{4K^2} - \frac{H''f_Q}{4HK} \\ &\quad - \frac{f_QH'K'}{4HK^2} - \frac{3f'_Q}{2Kr} + \frac{3f_QH'}{4HKr} \\ &\quad + \frac{f'_QK'}{4K^2} - \frac{2f_Q}{r^2} - \frac{f_QK'}{Kr^2} + \frac{f'_Q}{rK}, \\ \delta_{10} &= -\frac{3H'f_Q}{4HK} - \frac{2f'_Q}{K} \\ &\quad + \frac{f_QK'}{2K^2} - \frac{3f_Q}{2Kr} - \frac{f_Q}{rK}, \\ D_8 &= \frac{f}{2} - \frac{f_RR}{2} + \frac{f'_R}{rK} - \frac{2f_R}{r^2K} \\ &\quad + \frac{K'f'_R}{2K^2} - \frac{f''_R}{K} - \frac{H'f'_R}{2HK}, \\ Z &= \frac{2}{2 + Rf_Q + 2f_T} \left[\frac{f'_QPK'H'}{4K^2H} - \frac{f'_QPH'}{2HK} \right. \\ &\quad + \frac{f'_QPH'^2}{4KH^2} + \frac{f'_QPK'}{rK^2} + \frac{f_QPK''H'}{4HK^2} \\ &\quad + \left. \frac{3f_QPK'H''}{4HK^2} - \frac{f_QPH'''}{2HK} \right] \end{aligned}$$

$$\begin{aligned}
 & + \frac{f_Q P H'' H'}{4H^2 K} - \frac{f_Q P H'^3}{2KH^3} - \frac{f_Q P K''}{rK^2} - \frac{f_Q P K'}{r^2 K^2} \\
 & - \frac{f_Q P K'^2 H'}{2HK^3} + \frac{f_Q P' K' H'}{8K^2 H} \\
 & - \frac{f_Q P' H''}{4KH} + \frac{f_Q P' H'^2}{8KH^2} - P' f_T - P f'_T \\
 & + \frac{f_Q P'}{r^2 K} + \frac{f'_Q P H'}{K H r} + \frac{f'_Q P}{K r^2} + \frac{f_Q P' H'}{K H r} \\
 & - \frac{f_Q R' P}{2} - \frac{f'_Q R P}{2} + \frac{f_Q \rho' K' H'}{8K^2 H} - \frac{f_Q \rho' H''}{4KH} \\
 & + \frac{f_Q \rho' H'^2}{8KH^2} - \rho' f_T - \rho f'_T + \frac{\rho' f_T}{2} \\
 & - \left. \frac{P' f_T}{2} - \frac{f_Q \rho' H'}{2KHr} + \frac{f_Q P' H'}{2KHr} + \frac{f_Q \rho'}{r^2 K} \right].
 \end{aligned}$$

References

[1] P O Mazur and E Mottola, *Proc. Natl Acad. Sci. USA* **101**, 9545 (2004)
 [2] C Cattoen, T Faber and M Visser, *Class. Quantum Gravity* **22**, 4189 (2005)
 [3] M Visser and D L Wiltshire, *Class. Quantum Gravity* **21**, 1135 (2004)
 [4] A DeBenedictis, D Horvat, S Ilijic, S Kloster and K Viswanathan, *Class. Quantum Gravity* **23**, 2303 (2006)
 [5] C B Chirenti and L Rezzolla, *Class. Quantum Gravity* **24**, 4191 (2007)
 [6] N Sakai, H Saida and T Tamaki, *Phys. Rev. D* **90**, 104013 (2014)
 [7] S Fay, S Nesseris and L Perivolaropoulos, *Phys. Rev. D* **76**, 063504 (2007)
 [8] N J Poplawski, preprint [arXiv:gr-qc/0608031](https://arxiv.org/abs/gr-qc/0608031) (2006)
 [9] T Harko, F S N Lobo, S Nojiri and S D Odintsov, *Phys. Rev. D* **84**, 024020 (2011)
 [10] A Das, S Ghosh, D Deb, F Rahaman and S Ray, *Nucl. Phys. B* **954**, 114986 (2020)
 [11] U Debnath, *Eur. Phys. J. C* **79**, 499 (2019)
 [12] Z Haghani, T Harko, F S N Lobo, H R Sepangi and S Shahidi, *Phys. Rev. D* **88**, 044023 (2013)
 [13] S D Odintsov and D Sáez-Gómez, *Phys. Lett.* **725**, 437 (2013)
 [14] E Baffou, M Houndjo and J Tosssa, *Astrophys. Space Sci.* **361**, 376, (2016)

[15] I Ayuso, J B Jiménez and Á de la Cruz-Dombriz, *Phys. Rev. D* **91**, 104003 (2015)
 [16] Z Yousaf, M Bhatti and T Naseer, *Eur. Phys. J. Plus* **135**, 323 (2020)
 [17] Z Yousaf, M Bhatti and T Naseer, *Phys. Dark Universe* **28**, 100535 (2020)
 [18] M Z Bhatti, Z Yousaf and M Nawaz, *Int. J. Geom. Meth. Mod. Phys.* **17**, 2050017 (2020)
 [19] M Z Bhatti, K Bamba, Z Yousaf and M Nawaz, *J. Cosmol. Astropart. Phys.* **09**, 011 (2019)
 [20] Z Yousaf, M Bhatti and H Asad, *Phys. Dark Universe* **28**, 100527 (2020)
 [21] Z Yousaf, *Phys. Scr.* **97**, 025301 (2022)
 [22] Z Yousaf, *Universe* **8**, 131 (2022)
 [23] S Ghosh *et al*, *Phys. Lett. B* **767**, 380 (2017)
 [24] S Ghosh, S Ray, F Rahaman and B Guha, *Ann. Phys.* **394**, 230 (2018)
 [25] S Ghosh, D Shee, S Ray, F Rahaman and B K Guha, *Results Phys.* **14**, 102473 (2019)
 [26] S Ghosh, D Shee, S Ray, F Rahaman and B K Guha, *Ann. Phys.* **411**, 167968 (2019)
 [27] M Bhatti, Z Yousaf and M Ajmal, *Int. J. Mod. Phys. D* **28**, 1950123 (2019)
 [28] A Das, S Ghosh, B Guha, S Das, F Rahaman and S Ray, *Phys. Rev. D* **95**, 124011 (2017)
 [29] R Sengupta, S Ghosh, S Ray, B Mishra and S Tripathy, *Phys. Rev. D* **102**, 024037 (2020)
 [30] S Ray, R Sengupta and H Nimesh, *Int. J. Mod. Phys. D* **29**, 2030004 (2020)
 [31] Y B Zeldovich, *Mon. Not. R. Astron. Soc.* **160**, 1P (1972)
 [32] B J Carr, *Astrophys. J.* **201**, 1 (1975)
 [33] M S Madsen, J P Mimoso, J A Butcher and G F Ellis, *Phys. Rev. D* **46**, 1399 (1992)
 [34] P S Wesson, *Vistas Astron.* **29**, 281 (1986)
 [35] T M Braje and R W Romani, *Astrophys. J.* **580**, 1043 (2002)
 [36] L P Linares, M Malheiro and S Ray, *Int. J. Mod. Phys. D* **13**, 1355 (2004)
 [37] W Israel, *Nuovo Cimento B* **44**, 1 (1966)
 [38] G Darmonis, *Memorial des Sciences Mathématiques* (Gauthier Villars, Paris, 1927) Vol. 25
 [39] Z Yousaf, M Z-u-H Bhatti and U Farwa, *Eur. Phys. J. C* **77** 359 (2017)
 [40] K Lanczos, *Ann. Phys. (Berlin)* **379**, 518 (1924)
 [41] N Sen, *Ann. Phys. (Berlin)* **378**, 365 (1924)
 [42] G Perry and R B Mann, *Gen. Relativ. Gravit.* **24**, 305 (1992)
 [43] P Musgrave and K Lake, *Class. Quantum Gravity* **13**, 1885 (1996)